Science Advances
AAAS

advances.sciencemag.org/cgi/content/full/4/8/eaas9846/DC1

Supplementary Materials for

Microglial pannexin-1 channel activation is a spinal determinant of joint pain

Michael Mousseau, Nicole E. Burma, Kwan Yeop Lee, Heather Leduc-Pessah, Charlie H. T. Kwok, Allison R. Reid, Melissa O'Brien, Boriss Sagalajev, Jo Anne Stratton, Natalya Patrick, Patrick L. Stemkowski, Jeff Biernaskie, Gerald W. Zamponi, Paul Salo, Jason J. McDougall, Steven A. Prescott, John R. Matyas, Tuan Trang*

*Corresponding author. Email: trangt@ucalgary.ca

Published 8 August 2018, *Sci. Adv.* **4**, eaas9846 (2018)
DOI: 10.1126/sciadv.aas9846

This PDF file includes:

Fig. S1. MIA induces mechanical allodynia in rats.
Fig. S2. ATF3 and CSF1 expression in L3-L5 DRG is comparable in sham and MIA joint-injured rats on day 7.
Fig. S3. Microglial proliferation and Mac1-saporin depletion of spinal microglia.
Fig. S4. Characterization of microglial Panx1-deficient mice.
Fig. S5. Dynamic weight-bearing baseline quantification.
Fig. S6. Probenecid does not alter primary joint afferent activity.
Fig. S7. Probenecid alleviates ACLx-induced joint pain.

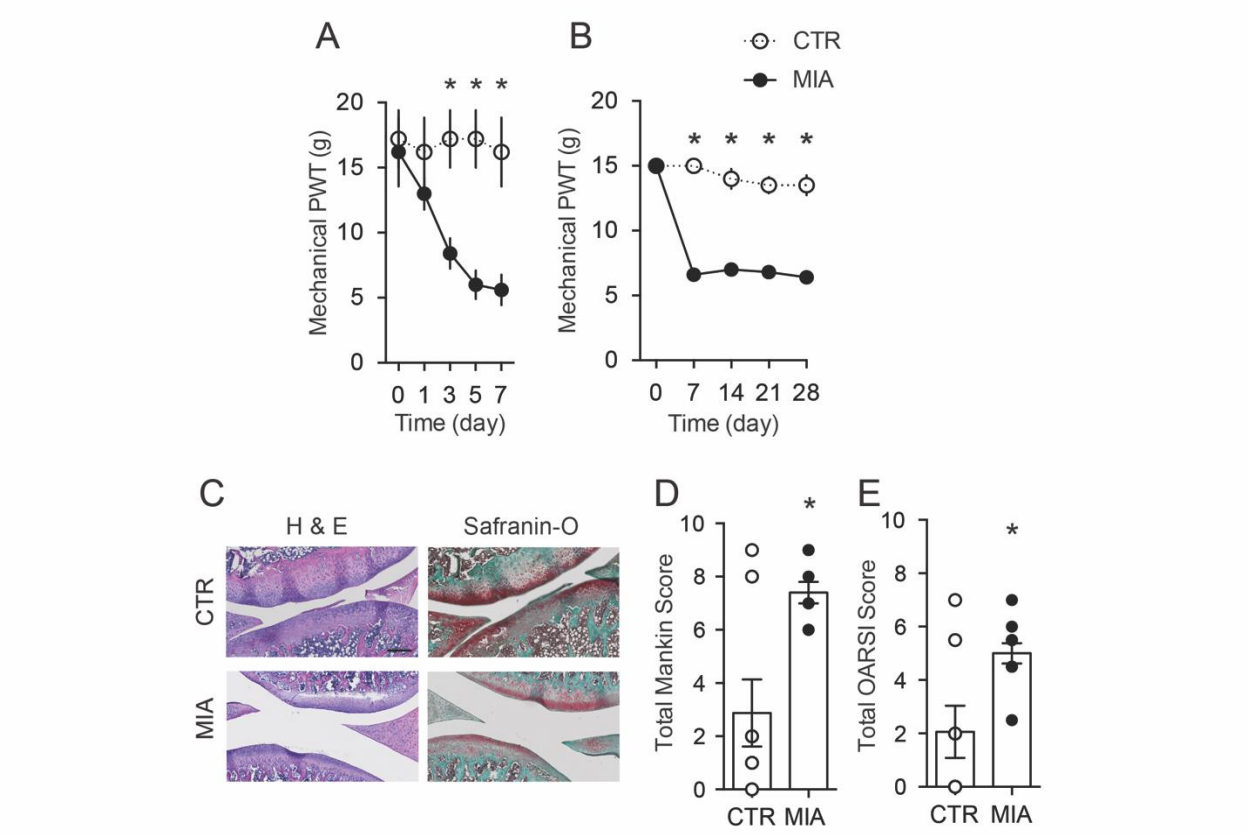

Fig. S1. MIA induces mechanical allodynia in rats. (**A**) Mechanical paw withdrawal threshold (PWT) measured daily in rats injected with intra-articular MIA (2 mg) or saline CTR (CTR, n=5; MIA, n=5). (**B**) Mechanical PWT measured up to 28 days post-MIA or saline (CTR) injection (CTR, n=10; MIA, n=10). (**C**) Cross sections (scale bar 100 μm) of rat knee joints with established arthritis were analyzed using the (**D**) modified Mankin scoring systems and (**E**) OARSI scoring systems to quantify arthritis pathology. (CTR, n=8; MIA, n=10). *p<0.05. Two-way repeated measures ANOVA (A and B) followed by Sidak post hoc test or unpaired t-test (D and E).

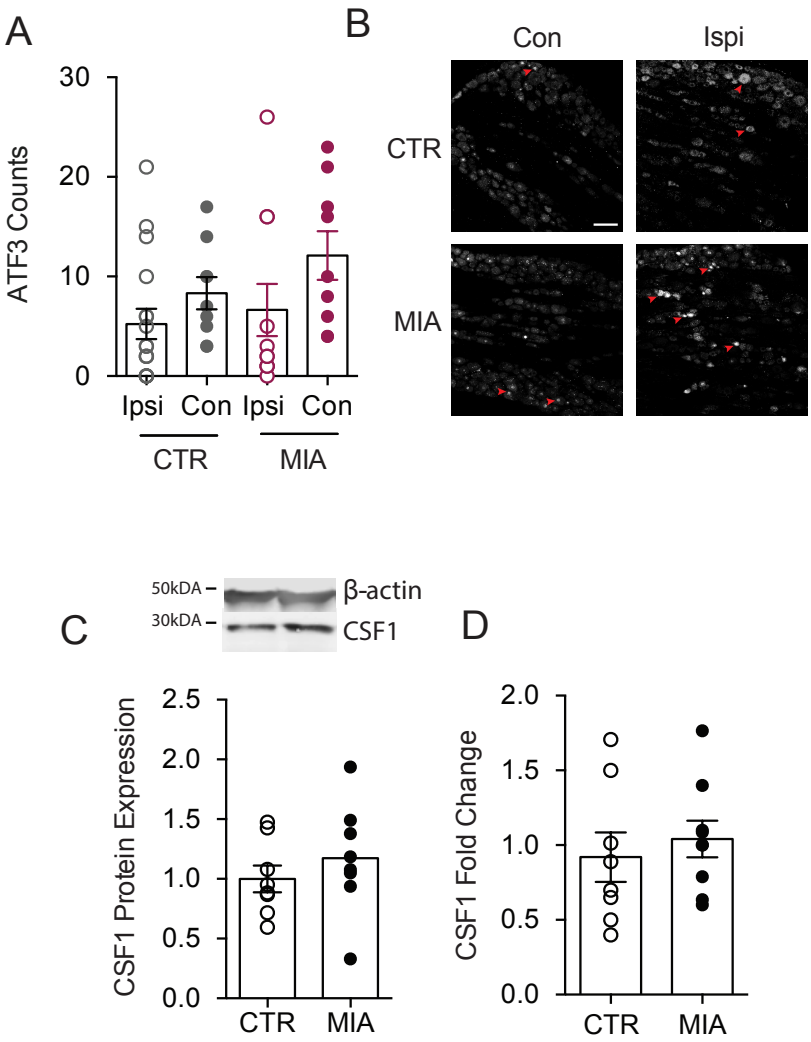

Fig. S2. ATF3 and CSF1 expression in L3-L5 DRG is comparable in sham and MIA joint-injured rats on day 7. (**A**) Quantification and (**B**) representative images of ATF3 positive cells from ipsilateral (Ipsi) and contralateral (Con) L3-L5 dorsal root ganglia of MIA and sham rats (CTR/Ipsi, n=17; CTR/Con, n=9; MIA/Ipsi, n=11; MIA/Con, n=9) (scale bar, 100 µm). One-Way ANOVA followed by Sidak post-hoc test. (**C**) CSF1 protein levels measured by Western blot (MIA: n=8; CTR: n=8), and (**D**) CSF1 mRNA by quantitative PCR (MIA: n=9; CTR: n=8) in L3-L5 dorsal root ganglia homogenates isolated from rats 7 days after intra-articular injection of MIA or saline. Primers for CSF1 were used to amplify cDNA, compared relative to housekeeping gene RPLP, and quantified using the delta Ct method. Unpaired t-test (C and D).

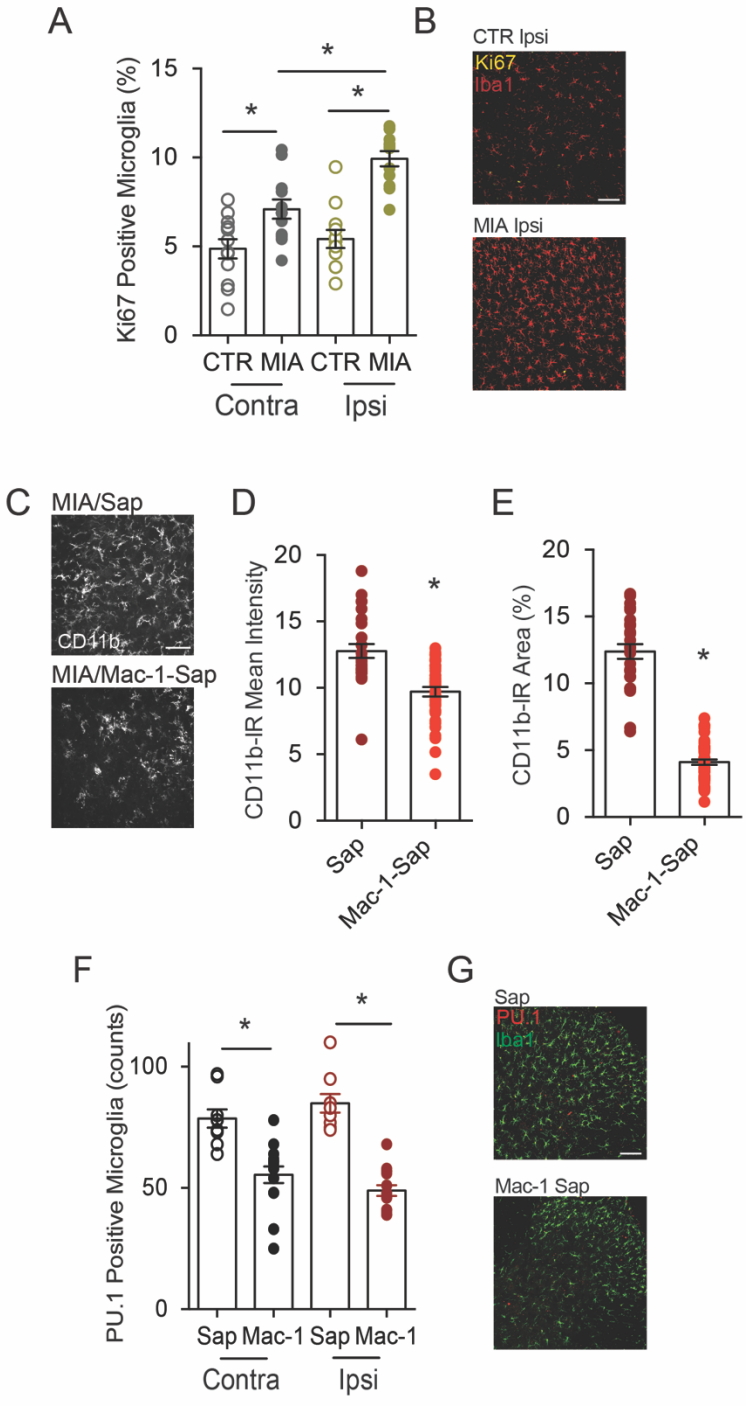
A
B
Ki67 Positive Microglia (%)
15
10
5
0
*
*
*
CTR MIA CTR MIA
Contra
Ipsi
CTR Ipsi
Ki67
Iba1
MIA Ipsi
C
MIA/Sap
CD11b
MIA/Mac-1-Sap
D
CD11b-IR Mean Intensity
20
15
10
5
0
*
Sap
Mac-1-Sap
E
CD11b-IR Area (%)
20
15
10
5
0
*
Sap
Mac-1-Sap
F
PU.1 Positive Microglia (counts)
100
50
0
*
*
Sap Mac-1 Sap Mac-1
Contra
Ipsi
G
Sap
PU.1
Iba1
Mac-1 Sap

Fig. S3. Microglial proliferation and Mac1-saporin depletion of spinal microglia. (**A**) Quantification and (**B**) representative images of microglia co-stained with the proliferation marker Ki67 and Iba1 in the L4-L5 lumbar segment spinal dorsal horn. Sections from MIA and CTR animals were imaged (n=12 for all groups). (**C**) Representative images and (**D** and **E**) quantification of CD11b immunoreactivity in the spinal dorsal horn of rats treated with Mac1-Saporin or saporin control. (Sap, n=26; Mac1-Sap, n= 39 spinal cord sections analyzed per group). (**F**) Quantification of Iba1 and PU.1 stained cells. (**G**) Representative images of spinal dorsal horn sections from Mac-1 saporin or saporin treated control rats (Sap/Con, n=9; Mac-1/Con, n=15; Sap/Ipsi, n=9; Mac-1/Ipsi, n=15). *$p<0.05$. One way ANOVA (A and F) Unpaired t-test (D and E) (scale bar, 100 μm).

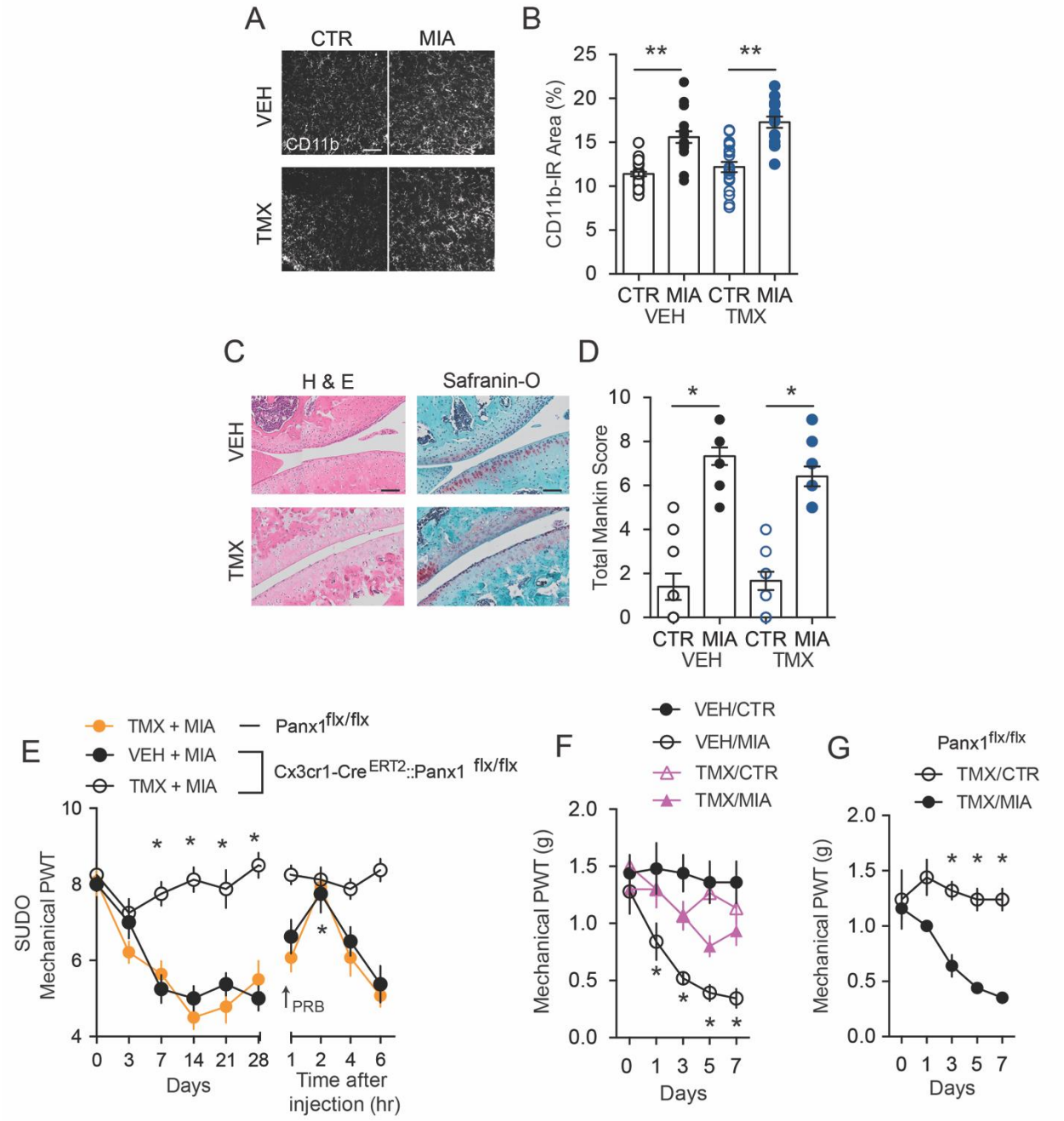
A
CTR
MIA
VEH
TMX
CD11b
B
CD11b-IR Area (%)
**
**
CTR MIA CTR MIA
VEH TMX
C
H & E
Safranin-O
VEH
TMX
D
Total Mankin Score
*
*
CTR MIA CTR MIA
VEH TMX
E
TMX + MIA
VEH + MIA
TMX + MIA
Panx1flx/flx
Cx3cr1-CreERT2::Panx1 flx/flx
SUDO Mechanical PWT
Days
PRB
Time after injection (hr)
F
VEH/CTR
VEH/MIA
TMX/CTR
TMX/MIA
Mechanical PWT (g)
Days
G
Panx1flx/flx
TMX/CTR
TMX/MIA
Mechanical PWT (g)
Days

Fig. S4. Characterization of microglial Panx1-deficient mice. (**A**) Representative images (scale bar 100 μm) and (**B** and **C**) quantification of CD11b immunofluorescence in the L3-L5 spinal dorsal horn from vehicle (VEH) or tamoxifen (TMX) treated *Cx3cr1*-Cre^{ERT2}::*Panx1*$^{flx/flx}$ mice after MIA (0.1 mg) or saline (CTR) injection. (VEH/CTR, n=31; VEH/MIA, n=17; TMX/CTR, n=20; TMX/MIA, n=15 spinal cord images per group). (C) Cross sections (scale bar, 100 μm) of *Cx3cr1*-Cre^{ERT2}::*Panx1*$^{flx/flx}$ mouse knee joints with established arthritis were analyzed using the (**D**) modified Mankin scoring systems to quantify arthritis pathology. (VEH/CTR, n=10; VEH/MIA, n=12; TMX/CTR, n=12; TMX/MIA, n=12). (**E**) Mechanical threshold in vehicle (VEH) and tamoxifen (TMX) *Cx3cr1*-Cre^{ERT2}::*Panx1*$^{flx/flx}$ treated mice and in Panx1$^{flx/flx}$ mice treated with TMX for 28 days followed by single i.p. injection of Probenecid (arrow) (100 mg/kg) on day 28 post MIA injection (Panx1$^{flx/flx}$: TMX/MIA, n=7. *Cx3cr1*-Cre^{ERT2}::*Panx1*$^{flx/flx}$: VEH/MIA, n=8; TMX/MIA, n=8). Mechanical PWT was assessed by von Frey filaments using the SUDO method. Baseline threshold in gram force is 1.1g. (**F**) Mechanical threshold in vehicle (VEH) and tamoxifen (TMX) Female *Cx3cr1*-Cre^{ERT2}::*Panx1*$^{flx/flx}$ treated mice (VEH/CTR, n=5; VEH/MIA, n=5; TMX/CTR, n=6; TMX/MIA, n=6). (**G**) Mechanical PWT measured daily in Panx1$^{flx/flx}$ mice treated with TMX 28 days prior to MIA or saline CTR injection (TMX/CTR; n=5, TMX/MIA; n=5). *p<0.05. **p<0.01. One-way ANOVA (B and D) or two-way repeated measures ANOVA (E-G) followed by Sidak post hoc test.

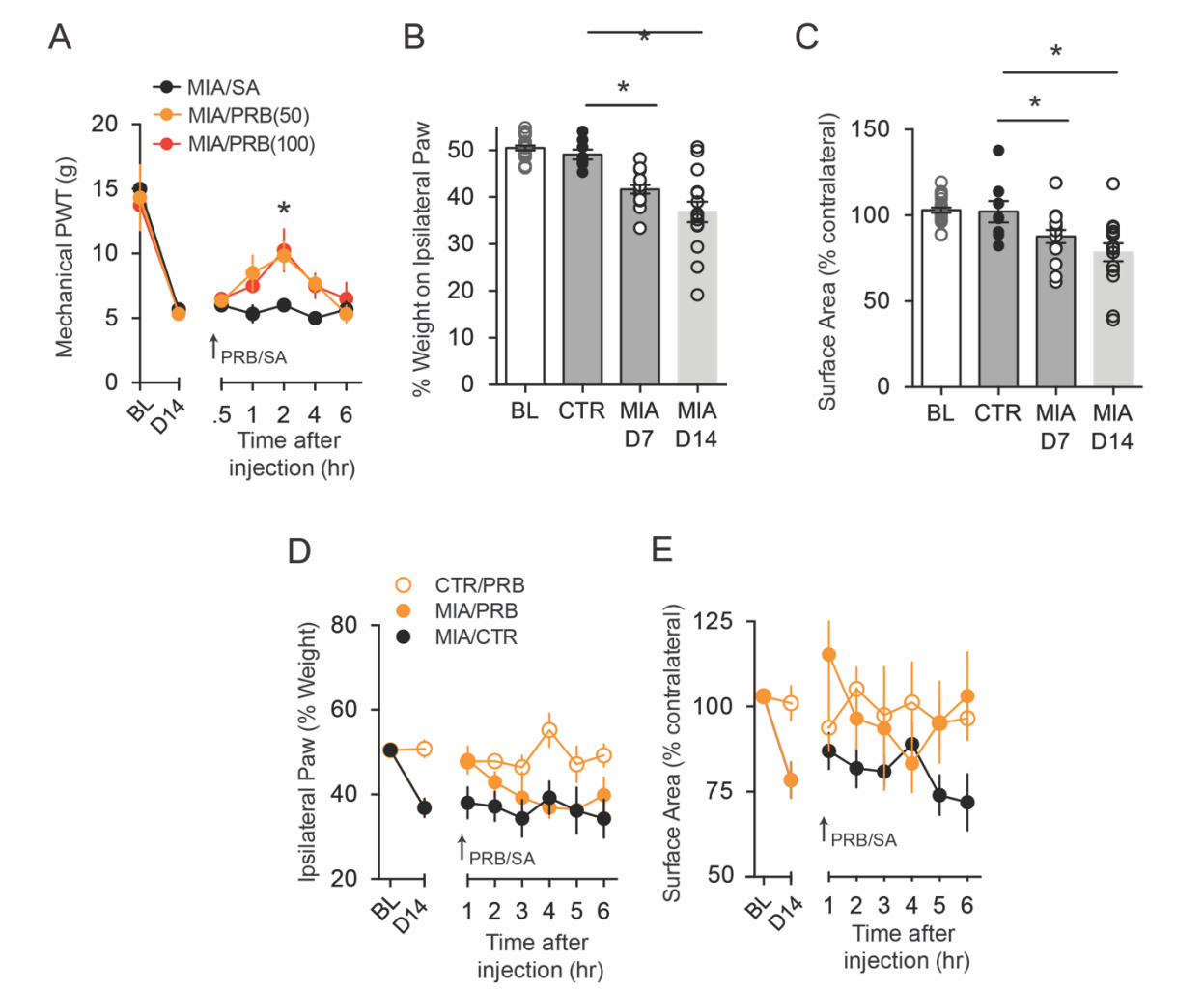

Fig. S5. Dynamic weight-bearing baseline quantification. (**A**) Mechanical paw withdrawal threshold (PWT) assessed by von Frey filament test on day 14 after MIA-induced joint injury (saline, n=6; PRB; 50 mg/kg: n=6, 100 mg/kg: n=4). Quantification of percent weight-bearing (**B**) and applied surface area (**C**) of the ipsilateral paw in rats at baseline, day 7 and day 14 post-MIA (2 mg) or saline (CTR) injection (Baseline (BL), n=23; Day 7/CTR, n=8; Day 7/MIA, n=15; Day 14/MIA, n=15). (**D** and **E**) Dynamic weight bearing assessed on day 14 after MIA-induced joint injury (CTR/PRB, n=8; MIA/PRB, n=7; MIA/Sal, n=8). Effect of PRB (50 mg/kg) on (D) weight bearing (day 14: $p = 0.0061$; Two-way ANOVA), and (E) paw surface area (day 14: $p = 0.0013$; Two-way ANOVA). Arrow represents single i.p. injection of PRB.*$p<0.05$. Two-way repeated measures ANOVA was performed (A, D and E). One-way ANOVA (B and C) followed by Sidak post hoc test.

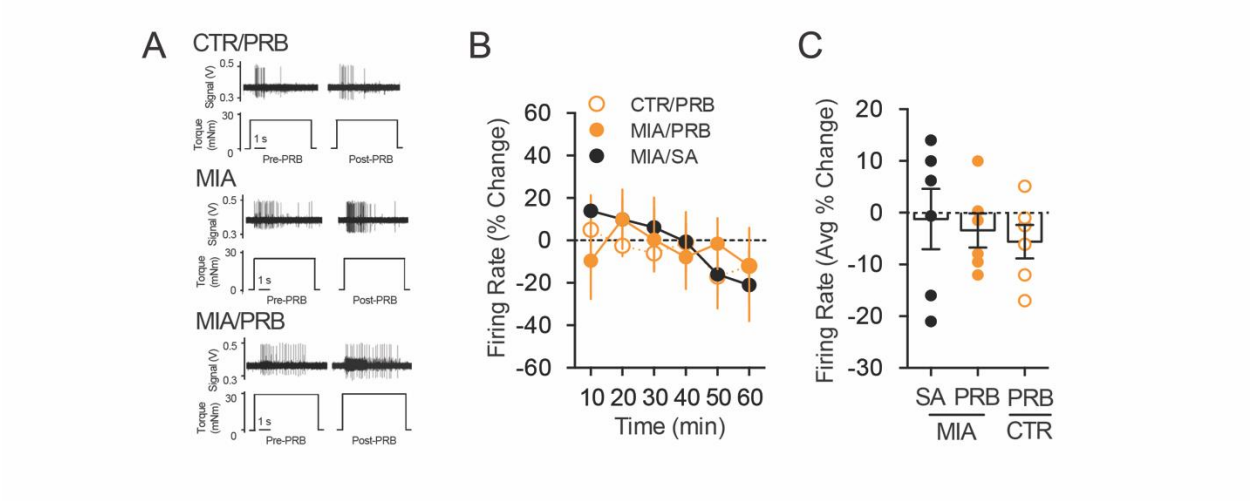

Fig. S6. Probenecid does not alter primary joint afferent activity. (**A**) Representative single-unit recordings from rat knee joint afferents pre- and post-probenecid (PRB) (50 mg/kg) i.p. injection in MIA and saline CTR animals. (**B**) Firing of rat knee joint afferents over 60 minutes after PRB treatment and (**C**) average percent change in firing rate at 60 minutes after PRB injection. (CTR/PRB, n=8; MIA/PRB, n=8; MIA/Sal, n=8). *p<0.05. Two-way repeated measures ANOVA (B and C) followed by Bonferroni post hoc test.

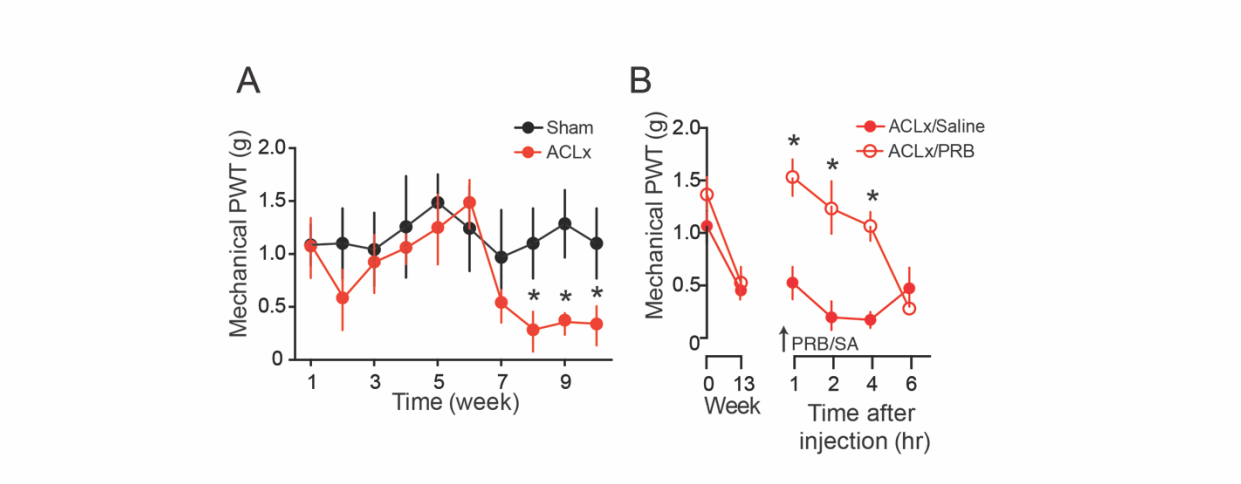

Fig. S7. Probenecid alleviates ACLx-induced joint pain. (**A**) Mechanical PWT measured up to 10 weeks post ACLx or sham surgery mice (Sham, n=7; ACLx, n=8). (**B**) Mechanical PWT following single injection of Probenecid i.p. (arrow) (100 mg/kg) 13 weeks post-surgery (ACLx/SA, n=3; ACLx/PRB, n=3). *p<0.05. Two-way repeated measures ANOVA (B and C) followed by Sidak post hoc test.